



Characterization and Influence of Porosity on the Two-Parameter Weibull Probability Distribution of Ceramic from Fired Clay

Muazu Abubakar
Department of Mechanical Engineering,
Bayero University, Kano, Nigeria

ABSTRACT

In this research, the characterization and influence of porosity on the two-parameter Weibull probability distribution of locally sourced clay were investigated. Characterization of the clay was conducted using XRF and XRD. The clay was mixed with 0%, 10%, and 15% wt starch to produce both dense and porous ceramics, which were then pressed and fired at 1300°C. The fired clay was characterized using XRD and FESEM. Some pore properties of the fired samples were determined using apparent porosity, bulk density, and BET. The flexural strength of the fired clay (33 samples each) was recorded using a three-point bending test. The flexural strength data were analyzed using a two-parameter Weibull probability distribution. From the XRF result, it is evident that silica and alumina are the major constituents in the clay. The XRD result shows that a mullite ceramic phase formed after firing at 1300°C. According to the Weibull probability results, the Weibull modulus increases (6.59-11.10) with increasing starch content. However, the scale parameter decreases (35.75-12.95 MPa) with increasing starch content. The FESEM results indicate that the dense fired clay exhibits a random orientation of cracks, while the porous ceramic shows a relative distribution of pores as the percentage of starch increases. This suggests that the clay can be utilized to produce both dense and porous ceramics for filtration and separation applications.

ARTICLE INFO

Article History
Received: August 2023
Received in revised form: September, 2023
Accepted: November, 2023
Published online: November, 2023

KEYWORDS

Weibull modulus; scale parameter; mullite; flexural strength

INTRODUCTION

Recently, due to its abundance, inexpensive clay minerals have received great attention in the production of ceramic-based materials used in novel areas such as membranes for separation and purification applications. An example of ceramic material that can be obtained from cheaply available clay minerals is mullite. Brittle materials under the same fabrication conditions tend to have variability in their mechanical properties especially flexural strength. This variability normally arises due to the susceptibility of these class of materials to cracks and porosity, which may arise from the production stage and become pronounced after subsequent firing. Flexural strength is considered the main mechanical

property to explain the strength of ceramic materials since they are weaker in tension than in compression (Della Bona *et al.*, 2003).

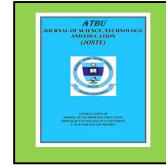
Failure strength in brittle materials are statistically distributed as a function of the flaw size distribution in the material (Della Bona *et al.*, 2003). Weibull probability distribution has been a tool to describe the structural reliability of ceramic materials. The parameters which describe the reliability of the ceramic materials are the Weibull modulus and the characteristic strength. Higher values of Weibull modulus show that the material has greater reliability. In addition, the characteristic strength represents failure strength at 63.2 percent of the tested materials. Generally, Weibull modulus of ceramic materials lies in the range $5 < m < 30$ (Yu *et al.*, 2009). In brittle

Corresponding author: Muazu Abubakar

✉ amuazu.mec@buk.edu.ng

Department of Mechanical Engineering, Bayero University, Kano.

© 2022. Faculty of Technology Education. ATBU Bauchi. All rights reserved



materials, sharp flaw such as microcracks are more sensitive to failure than blunt flaws such as pores (Quinn and Quinn, 2010)

Several researchers have used Weibull probability distribution to model the strength of brittle materials such as ceramics. For example, Della Bona *et al.*, (2003) researched veneered ceramics for dental restoration, and reported a weibull modulus in the range 5.20-14.10 and characteristics strength of 51.40-185.9 MPa. In similar research, Rodrigues *et al.*, (2007) reported a Weibull modulus in the range 7.6-13.10 and characteristic strength in the range 149.5-159.8 MPa when studying microhybrid and nanofil composites for dental restorations. Yu *et al.*, (2009) studied porous Si_3N_4 , a Weibull modulus value in the range 7.42–16.20 and characteristic strength of 103.30-184.09 MPa. Stawarczyk *et al.*, (2012) evaluated the flexural strength of hiped and pre-sintered zirconia for reconstructive dentistry; a Weibull modulus in the range 7.1-9.8 and characteristic strength in the range 984-1751MPa have been reported. In another research, Fan *et al.*, (2013) reported a Weibull modulus in the range 6.6-11.9 and characteristic strength in the range of 0.282-0.363 MPa when studying the fracture strength of high porous hydroxyapatite for biomedical applications. Furthermore, Thomason, (2013) studied the Weibull analysis of composites reinforced with fibres; a Weibull modulus value in the range 4.90-5.52 and a characteristic strength in the range of 3.62-3.80 has been reported.

Many studies have reported the Weibull modulus and characteristics strength of engineering ceramics. However, there is no detailed study of Weibull modulus and characteristics strength on dense and porous ceramics obtained from traditional clays. The objective of this work is to characterize the physical properties of local kaolinitic clay and evaluate the flexural strength of such clay using Weibull probability distribution.

MATERIALS AND METHODS

The clay was obtained from Getso Local Government of Kano state. The clay was washed to reduce the reddish-brown color of iron

oxide. The clay was sieved through 50 μm sieved with the aid of zirconia balls. The chemical composition determination by X-Ray Fluorescence technique (XRF) was conducted on the raw clay using Philips PW 2400 spectrometer. The different phases present in the raw clay and the fired clay at a temperature of 1300°C were determined by XRD using an automated Siemens Diffractometer D5000 equipment with Cu K α radiation source ($\lambda=1.5405\text{\AA}$) generated at 35 kV and 25 mA, at a step size angle of 0.05°, scan rate of 2° in 2 θ unit, and a scan range from 5 to 70°.

The composition by mass of each specimen was obtained by mass, density and volume relationship. To form the exact composition of each specimen, the percentage of starch (pore former) was added to the clay after subtracting the equivalent mass of the starch from the clay. To form the compacted specimens for the production of porous ceramic, the raw clay was mixed with starch in percentages of 0, 10 and 15wt% (specimens A, B, and C respectively); ethanol of 99.5% concentration for the wet mixing was added for the wet mixing of the specimens at 300 rpm. The mixing lasted for three hours, to ensure a homogenous mixture of clay and starch. After mixing, the mixture was dried in an oven for 24 hours at 80°C. The drying was conducted in order to evaporate the ethanol; the temperature was set so as not to burn the organic constituents present in the starch. Finally, the dried mixture was sieved through 100 μm sieve to ensure uniform distribution of the starch in the clay. The green samples for the flexural strength test were obtained by compaction and addition of glycerol as a binder in a mold of average span and width of 4 mm and 28.9 mm respectively.

The flexural strength of specimens A, B, and C fired at 1300°C were determined using a three-point bending test according to equation 1. The firing was done at 1300°C. The specimens' width and breadth were measured and recorded and a span of 40 mm was used for the test. A load was applied to the specimen until fracture. The test was conducted using cussons P5030 electro-mechanical testing machine at a

Corresponding author: Muazu Abubakar

✉ amuazu.mec@buk.edu.ng

Department of Mechanical Engineering, Bayero University, Kano.

© 2022. Faculty of Technology Education. ATBU Bauchi. All rights reserved

loading rate of 0.5 mm/min, based on ASTM C674-88, (1999).

$$\sigma = \frac{3PL}{2b^2d} \dots\dots(1)$$

Where P is the load applied, L is the test span length, d is the width and b is the thickness. The width of the specimens is within the range 3.2-3.5 mm and length of range 27.6-28.1 mm.

The least-square approach of the Weibull probability distribution was justified by linearizing the three-parameter Weibull cumulative distribution function equation by taking the double natural logarithm of equation 2 (ASTM C1239-131, 1-18).

$$P_i = 1 - \exp\left[-\left(\frac{\sigma - s}{\sigma_o}\right)^m\right] \dots\dots (2)$$

$$\ln[\ln(1/(1 - P_i))] = m \ln(\sigma - m \ln(\sigma_o - s)) \dots\dots (3)$$

For the two-parameter Weibull, the threshold stress is assumed zero, hence it reduces to equation 4:

$$\ln[\ln(1 / (1 - P_i))] = m \ln(\sigma) - m \ln(\sigma_o) \dots\dots (4)$$

To compute LS, each P_i of the specimen group was estimated by arranging the data from the smallest to the largest value i th position, which is the representative of the population percentage near to which the i th observation falls. Probabilities of failure for each group containing N specimens used are computed using the following equations:

Herd-Johnson (Mean Rank) is normally used for censored data, given by (Byun *et al.*, 2010; Bernard-granger *et al.*, 2011):

$$P_i = \frac{Q_i}{N + 1} \dots\dots (5)$$

The median rank method (Bernad) is considered the best estimator for the Y-plotting positions and is widely used for complete (uncensored (Petry *et al.*, 1997, Zhang *et al.*, 2006):

$$P_i = \frac{Q_i - 0.3}{N + 0.4} \dots\dots(6)$$

The Hazen method (modified Kaplan Meier) result is the least bias for $N \geq 20$ and probably the most preferable from a material science point of view, given by (Wu *et al.*, 2006; Gorjan and Ambrožič, 2012;Yatongchai *et al.*, 2013):

$$P_i = \frac{Q_i - 0.5}{N} \dots\dots(7)$$

Finally, the Kaplan Meier estimate has the following expression for uncensored data (Wang and Keats 1995):

$$P_i = \frac{Q_i}{N} \dots\dots (8)$$

The morphology of the fired compacted specimens was recorded using SEM.

RESULTS AND DISCUSSION

The chemical composition of the clay sieved through 50 μ m (Table 1) shows that alumina and silica are the major constituents of the clay. Other compounds present in the clay are potassium oxide (K₂O), iron oxide (Fe₂O₃), calcium oxide (CaO), titanium oxide (TiO₂), magnesium oxide (MgO), manganese oxide (MnO), potassium oxide (P₂O₅) and loss on ignition (LOI) of 11.54%. These are present in the clay as impurities.

Table 1: Chemical composition of Getso clay used in this research (wt%)

Compound	SiO ₂	Al ₂ O ₃	K ₂ O	Fe ₂ O ₃	CaO	TiO ₂	MgO	MnO	P ₂ O ₅	LOI
%wt	48.86	37.83	1.34	0.36	0.06	0.05	0.04	0.01	0.01	11.51

Fig. 1 shows the XRD of the raw and the sintered clays. The results show that kaolinite is the major phase present in the clay at two

intense diffraction peaks at 2θ values of 22.45 and 43.67° respectively, with quartz at 2θ value of 27.9, 35.7 and 41.7° respectively and with

Corresponding author: Muazu Abubakar

✉ amuazu.mec@buk.edu.ng

Department of Mechanical Engineering, Bayero University, Kano.

© 2022. Faculty of Technology Education. ATBU Bauchi. All rights reserved

traces of illite at 2θ values of 28.1° . The clay sintered at 1300°C shows mullite phase formed at diffraction angle 2θ of 22.5° and 27.9° and

crystalite phase at 58.7° as reported by Castelein, et al., 2001.

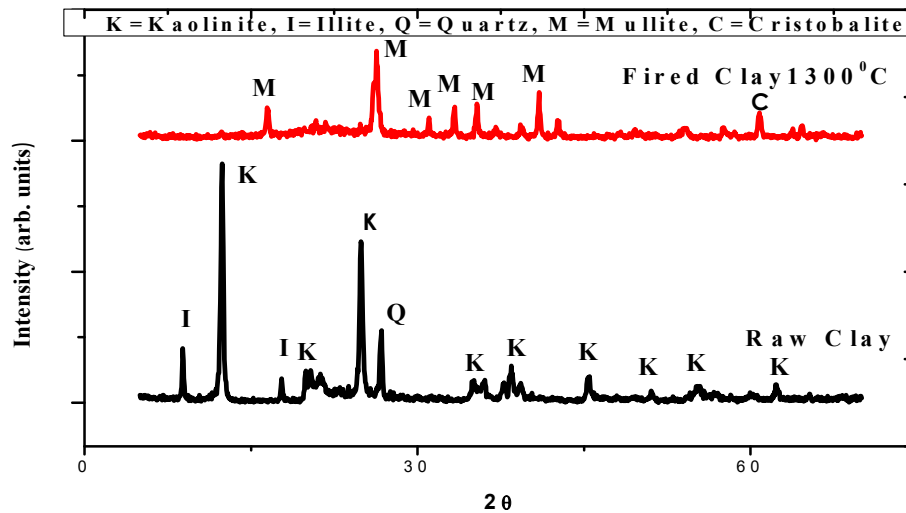


Figure 1: XRD analysis of the raw and sintered clay at 1300°C

The pore properties of the produced samples were presented in Table 2. From the table, it shows that the apparent porosity of fired samples increases with an increase in starch content. This is evident as the percentage starch increases, more voids will form after firing at 1300°C . However, the bulk density decreases as the percentage starch increases. This shows that as percentage starch increases, the higher the starch content, the more the population of voids/porosity is expected. The decrease in the bulk density is the consequence of an increase in internal void volume created as the result of the

starch burnout. The internal void volume created increases with the increasing percentage of starch initially in the specimens. Hence, this results in a decrease in bulk density. There is an inverse relationship between bulk density and apparent porosity; the higher the apparent porosity the lower the bulk density and vice versa. The pore surface area of the sample with higher starch content (sample C) has the highest surface area due to a large population of the voids as shown in Figure 4. Sample A shows no value of the pore surface area from BET results.

Table 2: Pore properties of the dense and porous ceramics fired at 1300°C

Sample	Apparent Porosity (%)	Bulk Density (g/cm^3)	Pore Surface Area (m^2/g)
A	5.94	2.47	-
B	19.56	1.93	1.28
C	27.15	1.68	1.71

Table 3 shows the flexural strength of specimens A, B and C at 1300°C using a three-point bending test. The flexural strength of specimens A, B and C depict variability in the

results under the same fabrication condition of pressure, time, composition and firing temperature, which further proves that brittle

Corresponding author: Muazu Abubakar

✉ amuazu.mec@buk.edu.ng

Department of Mechanical Engineering, Bayero University, Kano.

© 2022. Faculty of Technology Education. ATBU Bauchi. All rights reserved

materials under the same fabrication conditions have variability in their flexural strength.

Table 3: Flexural strength range of specimens A, B and C

Specimen	Minimum strength (MPa)	Maximum strength (MPa)	Range (MPa)
A	24.11	46.56	22.45
B	13.58	23.26	9.68
D	9.99	15.30	5.31

The scatter plot of $\ln[\ln(1/(1-p))]$ vs. $\ln(\sigma)$ for the different probability of failure estimates (mean, median, modified Kaplan Meier and Kaplan Meier) for two-parameter Weibull is presented in Figure 2. Among the plots, Figure 2d, which represents Kaplan Meier, gives the best fit for specimens A, B and C. In the Figure, all the probability points lie close to the line of best fit, while Figures 2a, 2b and 2c have more

probability points away from the line of best fit. Also, linear regression chases the lower strength data points, but lower and upper confidence interval bounds are not available in linear regression. One of the disadvantages of linear regression is the absence of upper and lower bounds of the confidence interval levels as reported by Stawarczyk *et al.*, 2012; Roos and Stawarczyk, 2012.

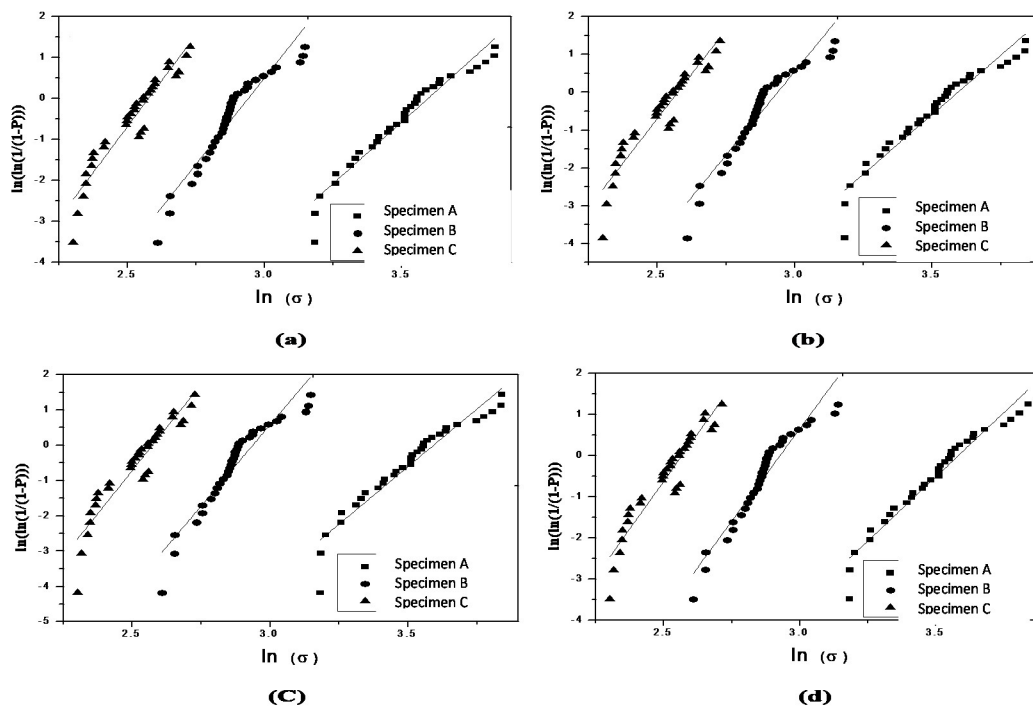


Figure 2: Two-parameter Weibull probability plot of specimens A, B and C (a) Mean (b) Median (c) Modified Kaplan Meier and (d) Kaplan Meier estimates

Table 4 shows the summary of Weibull modulus, characteristic strength and correlation coefficient of the various estimates. From Table

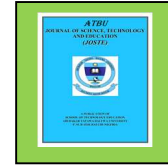
2, Kaplan Meier estimate shows the highest value of the correlation coefficient for the dense

Corresponding author: Muazu Abubakar

✉ amuazu.mec@buk.edu.ng

Department of Mechanical Engineering, Bayero University, Kano.

© 2022. Faculty of Technology Education. ATBU Bauchi. All rights reserved



(0.980) and porous (0.96 and 0.94) ceramic compared with the other estimates.

Fig. 2 is the probability plot of the Kaplan Meier estimates for the dense and the porous ceramic with the equations of estimating

the Weibull parameters. The high value of the correlation coefficient of the Kaplan Meier estimate makes it a suitable tool for estimating the Weibull parameters of the dense and the porous ceramic.

Table 4: Two-parameter Weibull parameters linear regression estimate

Estimate	Material	<i>m</i>	σ_0 (MPa)	R ²
Mean Rank (Herd-Johnson)	Specimen A	7.00	34.31	0.96
	Specimen B	9.42	16.76	0.94
	Specimen C	9.98	11.13	0.93
Median Rank (Bernad)	Specimen A	7.29	34.26	0.97
	Specimen B	9.85	16.65	0.94
	Specimen C	10.41	11.12	0.93
Kaplan Meier	Specimen A	7.24	33.81	0.98
	Specimen B	9.98	16.76	0.96
	Specimen C	10.28	11.20	0.94
Modified Kaplan Meier (Hazen)	Specimen A	7.53	34.26	0.95
	Specimen B	7.32	16.90	0.93
	Specimen C	7.45	11.21	0.93

The probability density function, Figure 3, represents the plot of density functions of specimens A, B and C for two-parameter Weibull probability distribution. Figure 3a shows that the probability density plot of specimen C gives narrowest flexural strength distribution due to its high value of the Weibull modulus followed by specimen B, while specimen A has a more spread distribution due to the low value of the Weibull modulus. The wider spread of the probability density is due to a random distribution of cracks which resulted in the scattering of the flexural strength. The narrow spread of the probability density is due to the relative distribution of porosity in the morphology of specimens B and C which gives a narrow distribution of the flexural strength. This makes the Weibull modulus of the porous ceramic

higher and reflected by the narrow distribution of the probability density plot. This observation has good agreement with previous studies (Roos and Stawarczyk, 2012). The narrower distribution curve suggests less variability in the flexural strength of the porous ceramic and high chances of predicting failure. Specimens A, B and C show skewness to the right of the probability density graph. The skewness in the distributions has a population concentrated at a value close to the scale parameter. The probability density function Kaplan Meier using linear regression is shown in Figure 2. From the results, Kaplan Meier has presented the best estimate to model the variability in flexural strength of both dense and porous ceramics produce from the clay as both the results of R² and the scatter plot gives the best fit for the estimate.

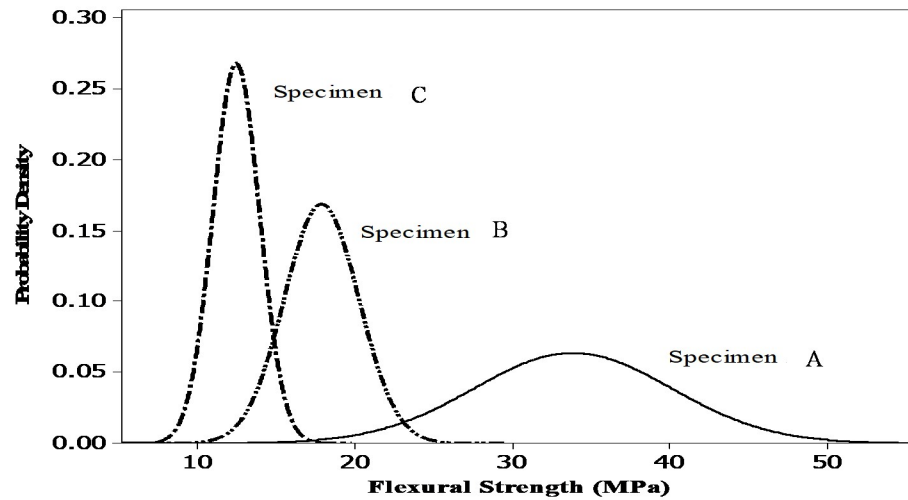


Figure 3: Probability density plot of specimen (A), (B) and (C)

The micrographs of fractured surfaces of specimens A, B and C fired at 1300°C are shown in Figure 4. From the micrograph, it can be depicted that specimen A contains random distribution of cracks (Figure 4a) while specimens B and C contain relative distribution of porosity (Figures 4b and 4c). This will result in variability in mechanical properties, which need to be modeled with Weibull probability distribution. The fractography analysis of porous ceramic at 1300°C of specimen B shows relative distribution of porosity and specimen C shows a partial distribution of porosity. This implies that

specimens B and C have a single distinct flaw distribution (porosity). This makes the data of the flexural strength uncensored (failure characterized by a single flaw) and suitable to apply Weibull probability distribution without applying methods associated with censored data (ASTM C1239-13, 2013). In addition, it shows that blunt flaws such as pores will result in high value of Weibull modulus compared with dense ceramic which has microcracks. This shows that predicting failure in porous ceramics is higher compared with the dense ceramic.

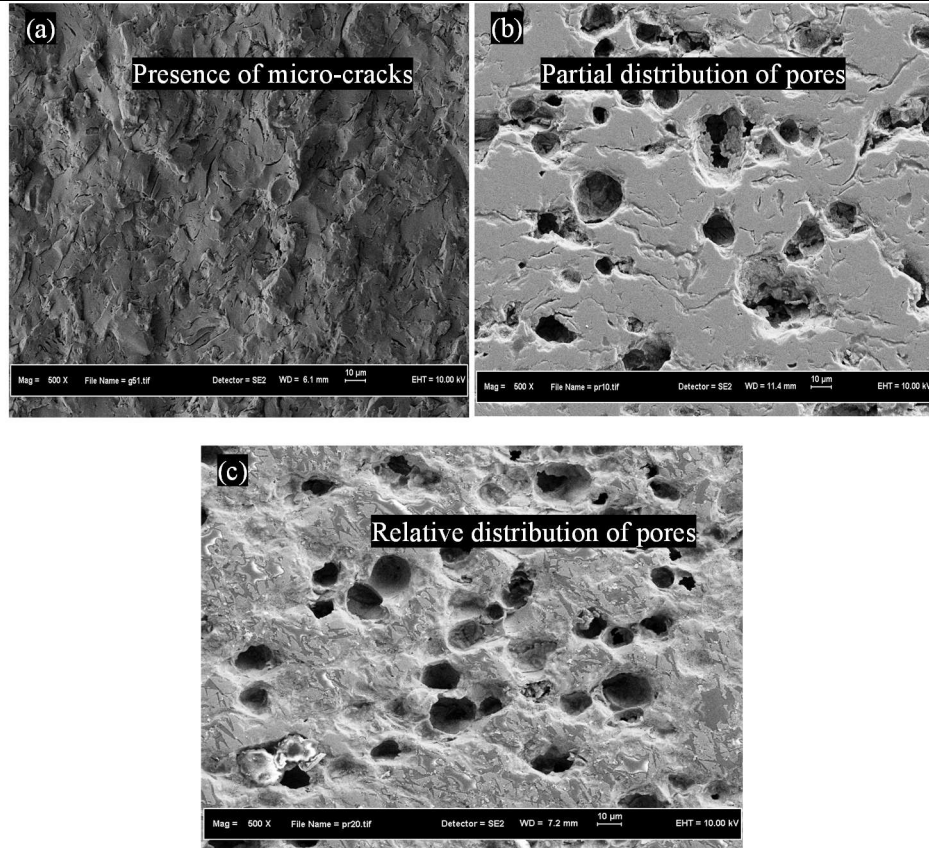


Figure 4: Fractured surface morphology of fired specimens (a) A (b) B and (c) C fired at 1300°C

CONCLUSION

This study demonstrates the viability of utilizing cost-effective clay as a source for mullite ceramics, enabling the production of both dense and porous ceramics from the same clay source. The Kaplan-Meier estimates prove to be the most suitable model for characterizing the flexural strength of both dense and porous ceramics. The Weibull modulus obtained for both types of ceramics falls within the range typical for ceramic materials.

The characteristic strength, representing the strength at which 63.2% of the materials will fail, is a key parameter. The porous ceramics exhibit higher Weibull modulus values due to the presence of pores, in contrast to the dense ceramic. The fractured morphology of the dense ceramic reveals a random distribution of

cracks, contributing to a lower Weibull modulus value. However, as the percentage of starch increases, the Weibull modulus demonstrates an upward trend, attributed to a more uniform distribution of pores in the porous ceramics. This indicates that the introduction of starch influences the distribution of pores, leading to enhanced mechanical properties in the resulting ceramics.

REFERENCE

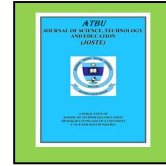
- ASTM (1999b) Standard Test Methods for Flexural Properties of Ceramic Whiteware Materials. ASTM C674-88. 1–19.
- ASTM (2014), Standard Practice for Reporting Uniaxial Strength Data and Estimating Weibull Distribution Parameters for

Corresponding author: Muazu Abubakar

✉ amuazu.mec@buk.edu.ng

Department of Mechanical Engineering, Bayero University, Kano.

© 2022. Faculty of Technology Education. ATBU Bauchi. All rights reserved



- Advanced Ceramics, ASTM C1239-131, 1–18.
- Bernard-granger, G., Guizard, C., and Monchalin, N. (2011) firing of an Ultrapure α -Alumina Powder : II. Mechanical, Thermo-Mechanical, Optical Properties, and Missile Dome Design. 382, 366–382.
- Byun, T. S., Hunn, J.D., Miller, J.H., Snead, L.L., and Kim, J.W. (2010) Evaluation of Fracture Stress for the SiC Layer of TRISO-Coated Fuel Particles Using a Modified Crush Test Method. 337, 327–337.
- O. Castelein, B. Soulestin, J. P. Bonnet, and P. Blanchart (2001). The influence of heating rate on the thermal behaviour and mullite formation from a kaolin raw material. *Ceramic International*, 27, pp.517–522.
- Della Bona, A., Anusavice, K.J., and DeHoff, P.H. (2003) Weibull analysis and flexural strength of hot-pressed core and veneered ceramic structures. *Dental Materials*, 19, 662–669.
- Fan, X., Case, E.D., Gheorghita, I., and Baumann, M.J. (2013) Weibull modulus and fracture strength of highly porous hydroxyapatite. *Journal of the mechanical behavior of biomedical materials*, 20, 283–95. Elsevier.
- Gorjan, L. and Ambrožič, M. (2012) Bend strength of alumina ceramics: A comparison of Weibull statistics with other statistics based on very large experimental data set. *Journal of the European Ceramic Society*, 32, 1221–1227.
- Petry, M. D., Mah, T., and Kerans, R. J. (1997) Validity of Using Average Diameter for Determination of Tensile Strength and Weibull Modulus of Ceramic Filaments. *Journal of American Ceramic Society* 44, 2741–2744.
- Quinn, J.B. and Quinn, G.D. (2010) A practical and systematic review of Weibull statistics for reporting strengths of dental materials. *Dental materials : official publication of the Academy of Dental Materials*, 26, 135–47.
- Rodrigues, S.A., Ferracane, J.L., and Bona, D. (2007) Flexural strength and Weibull analysis of a microhybrid and a nanofill composite evaluated by 3- and 4-point bending tests. 4, 426–431.
- Stawarczyk, B., Ozcan, M., Trottmann, A., Hämmerle, C.H.F., and Roos, M. (2012) Evaluation of flexural strength of hiped and presintered zirconia using different estimation methods of Weibull statistics. *Journal of the mechanical behavior of biomedical materials*, 10, 227–34. Elsevier Ltd.
- Thomason, J.L. (2013) On the application of Weibull analysis to experimentally determined single fibre strength distributions. *Composites Science and Technology*, 77, 74–80.
- Yu, F., Yang, J., Xue, Y., Du, J., Lu, Y., and Gao, J. (2009) Effects of talc and clay addition on pressureless sintering of porous Si_3N_4 ceramics. *Bulletin of Materials Science*, 32, 177–181.
- Wang, F. K. and Keats, J. B. (1995) Improved Percentile Estimation for the Two-Parameter Weibull Distribution. *Microelectron Reliability*. 35, 883-892.
- Wu, D., Zhou, J., and Li, Y. (2006) Unbiased estimation of Weibull parameters with the linear regression method. *Journal of the European Ceramic Society*, 26, 1099–1105.
- Yatongchai, C., Wren, A. W., Curran, D. J., Hornez, J. C., and Mark R, T. (2013) Comparison of the Weibull characteristics of hydroxyapatite and strontium doped hydroxyapatite. *Journal of the mechanical behavior of biomedical materials*, 21, 95–108.
- Zhang, L. F., Xie, M., and Tang, L. C. (2007) A study of two estimation approaches for parameters of Weibull distribution based on WPP. *Reliability Engineering & System Safety*, 92, 360–368.

Corresponding author: Muazu Abubakar

✉ amuazu.mec@buk.edu.ng

Department of Mechanical Engineering, Bayero University, Kano.

© 2022. Faculty of Technology Education. ATBU Bauchi. All rights reserved